

# Synthesis of Ultra-incompressible $sp^3$ -Hybridized Carbon Nitride with 1:1 Stoichiometry

Elissaios Stavrou,<sup>\*,†,‡</sup> Sergey Lobanov,<sup>†,§</sup> Huafeng Dong,<sup>||</sup> Artem R. Oganov,<sup>||,⊥,#,▽</sup> Vitali B. Prakapenka,<sup>○</sup> Zuzana Konôpková,<sup>◆</sup> and Alexander F. Goncharov<sup>\*,†,¶,□</sup>

<sup>†</sup>Geophysical Laboratory, Carnegie Institution of Washington, Washington, DC 20015, United States

<sup>‡</sup>Lawrence Livermore National Laboratory, Physical and Life Sciences Directorate, P.O. Box 808, L-350, Livermore, California 94550, United States

<sup>§</sup>Sobolev Institute of Geology and Mineralogy Siberian Branch Russian Academy of Sciences, 3 Pr. Ac. Koptyga, Novosibirsk 630090, Russia

<sup>||</sup>Department of Geosciences, Center for Materials by Design, Institute for Advanced Computational Science, Stony Brook University, Stony Brook, New York 11794-2100, United States

<sup>⊥</sup>Skolkovo Institute of Science and Technology, Skolkovo Innovation Center, 5 Nobel St., Moscow 143026, Russia

<sup>#</sup>Moscow Institute of Physics and Technology, 9 Institutskiy Lane, Dolgoprudny City, Moscow Region 141700, Russia

<sup>▽</sup>School of Materials Science, Northwestern Polytechnical University, Xi'an 710072, China

<sup>○</sup>Center for Advanced Radiation Sources, University of Chicago, Chicago, Illinois 60637, United States

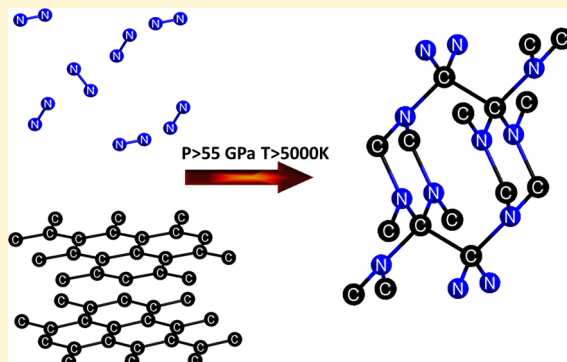
<sup>◆</sup>DESY Photon Science, D-22607 Hamburg, Germany

<sup>¶</sup>University of Science and Technology of China, Hefei 230026, China

<sup>□</sup>Key Laboratory of Materials Physics and Center for Energy Matter in Extreme Environments, Institute of Solid State Physics, Chinese Academy of Sciences, Hefei 230031, China

## S Supporting Information

**ABSTRACT:** The search of compounds with  $C_xN_y$  composition holds great promise for creating materials which would rival diamond in hardness due to the very strong covalent C–N bond. Early theoretical and experimental works on  $C_xN_y$  compounds were based on the hypothetical structural similarity of predicted  $C_3N_4$  phases with known binary  $A_3B_4$  structural types; however, the synthesis of  $C_3N_4$  other than g- $C_3N_4$  remains elusive. Here, we explore an “elemental synthesis” at high pressures and temperatures in which the compositional limitations due to the use of precursors in the early works are substantially lifted. Using *in situ* synchrotron X-ray diffraction and Raman spectroscopy, we demonstrate the synthesis of a highly incompressible  $Pnnm$  CN compound ( $x = y = 1$ ) with  $sp^3$ -hybridized carbon above 55 GPa and 7000 K. This result is supported by first-principles evolutionary search, which finds that CN is the most stable compound above 14 GPa. On pressure release below 6 GPa, the synthesized CN compound amorphizes, maintaining its 1:1 stoichiometry as confirmed by energy-dispersive X-ray spectroscopy. This work underscores the importance of understanding the novel high-pressure chemistry laws that promote extended 3D C–N structures, never observed at ambient conditions. Moreover, it opens a new route for synthesis of superhard materials based on novel stoichiometries



## INTRODUCTION

Since the pioneering work of Liu and Cohen<sup>1</sup> introducing a new class of highly incompressible solids, the search for  $C_3N_4$  materials harder than diamond has become the holy grail in the field of superhard materials. The original proposal was based on realization that carbon atoms in a hypothetical  $C_3N_4$  compound in the  $\beta$ - $Si_3N_4$  structure are bonded to 4 nitrogen atoms by very strong C–N bonds, which are shorter in comparison to the C–C bond in diamond (1.47 vs 1.53 Å at ambient pressure), and

the material is of low ionicity. In the subsequent work of Teter and Hemley,<sup>2</sup> a number of structures with similar bonding properties have been proposed. These structures, with the exception of the graphite-like g- $C_3N_4$ , have the  $sp^3$  bonding for C and N atoms, with the formation of  $CN_4$  corner-sharing

Received: June 27, 2016

Revised: August 31, 2016

Published: September 2, 2016



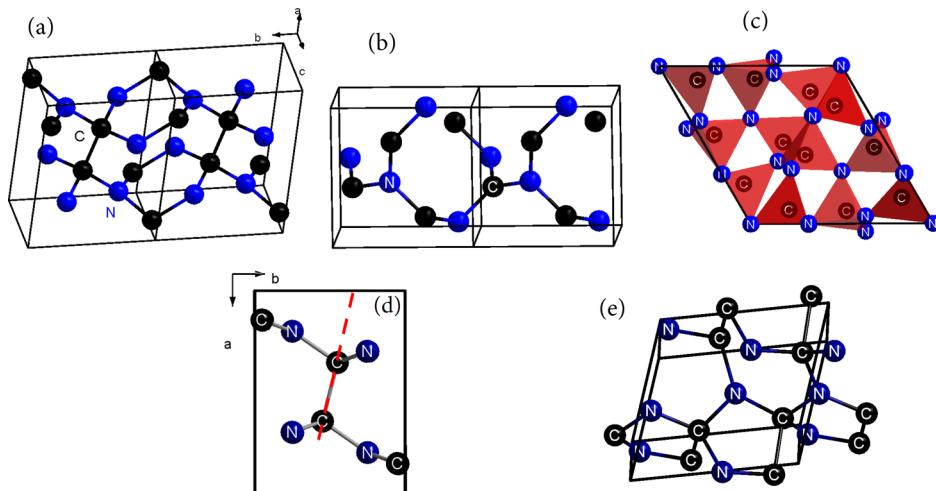


**Figure 1.** Schematic representations of (a)  $\beta$ -InS-type crystal structure of CN, (b) cg-CN, (c)  $\alpha$ -Si<sub>3</sub>N<sub>4</sub>-type crystal structure of C<sub>3</sub>N<sub>4</sub>, (d)  $\beta$ -InS-type crystal structure of CN viewed along *c* axis (the tilting of the C–C bond with respect to the *a* axis is highlighted by the red dashed line), and (e) monoclinic *Pc* crystal structure of CN. Black and blue spheres indicate carbon and nitrogen atoms, respectively.

tetrahedra (see Figure 1c) where C atoms are connected with 4 N atoms and N atoms with 3 C atoms. The bulk moduli of these compounds have been calculated (using DFT) to be very high, for some structures exceeding that of diamond, and, moreover, revealing very high densities and the presence of wide optical band gaps ( $>3$  eV). These early predictions were based on the structural similarity with known A<sub>3</sub>B<sub>4</sub> structural types, but for materials with atomic substitution. For instance,  $\alpha$ - and  $\beta$ -C<sub>3</sub>N<sub>4</sub><sup>2</sup> are analogues to  $\alpha$ - and  $\beta$ -Si<sub>3</sub>N<sub>4</sub>, respectively; while cubic C<sub>3</sub>N<sub>4</sub> is analogous to Th<sub>3</sub>P<sub>4</sub>.

These first theoretical predictions triggered extensive experimental and theoretical studies aiming at the synthesis of such unique covalent compounds. These attempts involved mainly the use of chemical precursors, such as, for instance, triazine (C<sub>3</sub>N<sub>3</sub>H<sub>3</sub>) based compounds, to synthesize C<sub>3</sub>N<sub>4</sub> phases through various mechanochemical techniques usually in the form of thin films and nanocrystals. Following this route, the synthesis of  $\alpha$ ,<sup>3</sup>  $\beta$ ,<sup>4–6</sup> and mainly g-C<sub>3</sub>N<sub>4</sub><sup>7,8</sup> had been reported, but these results were subsequently disputed as the identification of their structures was often ambiguous due to the limited quantity and heterogeneity of samples. Moreover, it appears that shock compression of the precursor materials results in diamond-like carbon containing nitrogen only at the impurity level.<sup>9,10</sup> The synthesis of a cubic C<sub>3</sub>N<sub>4</sub> phase, diverse (less dense) from the theoretically predicted,<sup>2</sup> has been reported<sup>11</sup> using high pressure and temperature conditions in the diamond anvil cell (DAC) experiments, but these results have not been confirmed by other studies, and moreover, large-volume press synthesis in similar conditions resulted in preferable diamond production.<sup>12</sup> In addition, although some new “C<sub>3</sub>N<sub>4</sub>” phases have been reported starting from g-C<sub>3</sub>N<sub>4</sub>, these observations could be due to the presence of hydrogen in starting compounds.<sup>13</sup>

The assumption about the 3:4 stoichiometry of the high-pressure hypothetical phases has been challenged by Cote and Cohen,<sup>14</sup> who realized that the original proposal based on the 3:4 composition does not gain experimental support. Indeed, *a priori*, the most stable composition for the C<sub>x</sub>N<sub>y</sub> materials at high pressures is unclear because carbon can exist in both sp<sup>2</sup>- and sp<sup>3</sup>-hybridized states. Therefore, carbon nitrides with 1:1 stoichiometry (CN) have been theoretically proposed<sup>14</sup> as more stable than the C<sub>3</sub>N<sub>4</sub> compounds at elevated pressures. As

in the case of C<sub>3</sub>N<sub>4</sub>, initial theoretical predictions for the CN compound<sup>14–16</sup> were based on known structural types of AB compounds like zincblende, rocksalt, body-centered tetragonal (bct), etc. More recent theoretical studies,<sup>17–19</sup> based on advanced structure prediction algorithms, have proposed additional CN crystal structures including a cg-CN,<sup>17</sup> an orthorhombic *Pnnm* CN,<sup>18</sup> and a tetragonal *P4<sub>2</sub>/m* with very similar to *Pnnm* CN structural characteristics.<sup>19</sup> It is noteworthy that the predicted *Pnnm* structure is identical with the  $\beta$ -InS, which has been proposed as the most energetically favored structure by Hart et al.<sup>15</sup> based on DFT calculations of the known structural types. For the CN 1:1 compound composition, carbon can be in either sp<sup>2</sup> or sp<sup>3</sup> configurations with C atoms connected with 3 N atoms or 3 N and 1 C atom, respectively. Representative phases of each family of CN materials are cg-CN and  $\beta$ -InS for sp<sup>2</sup>- and sp<sup>3</sup>-hybridized carbon, respectively (Figure 1). Superhard materials (hardness H > 40 GPa) are expected to occur for both bonding schemes (cg-CN,  $\beta$ -InS), as opposed to elemental carbon, which is superhard for the sp<sup>3</sup> bonding scheme only. As described in detail by Hart et al., the CN “sp<sup>3</sup> family” arises from alternating C and N around graphite rings (see Figure 1a) with additional C–C bonding between the sheets. These interlayer bonds may be between pairs of sheets, resulting in the layered GaSe-like CN structure,<sup>15</sup> or between multiple sheets, forming a 3D network as in  $\beta$ -InS.

Low dimensionality C<sub>x</sub>N<sub>y</sub> compounds with covalent C–N bonds are known to exist at ambient conditions as in the case of heterocyclic compounds such as pyridine and triazol. Pressure-induced polymerization, toward the formation of 2D layered structures, has been reported in the case of cyanide monomers.<sup>20</sup> However, solid evidence of a subsequent formation of a C<sub>x</sub>N<sub>y</sub> 3D network is still missing. Thus, the possible formation of a compound with covalent C–N single bonds forming a 3D network framework would represent a completely new chemical behavior.

Experimentally, in this study, we focus on an “elemental synthesis” by not restricting the *initial* compositions of the reagents (as opposed to using chemical precursors) and also using very clean hydrogen-free techniques; we apply only thermodynamic stimuli (pressure and temperature), using a standard laser-heated (LH) DAC configuration, attempting to

grow the most stable material irrespectively of the composition. We report the experimental synthesis of a *Pnnm* ( $\beta$ -InS) CN phase under high-pressure and high-temperature conditions examined by *in situ* high  $P$ – $T$  visual observations, synchrotron X-ray diffraction (XRD), Raman confocal spectroscopy, and also energy-dispersive X-ray spectroscopy (EDX) probes at ambient conditions. We stress that pressure is the necessary thermodynamic stimulus for the synthesis of  $C_xN_y$  compounds, regardless of their structure and composition. Previous theoretical studies have indicated a ca. 10–15 GPa threshold above which  $C_xN_y$  compounds become thermodynamically stable with respect to decomposition into elemental carbon and nitrogen.<sup>18</sup> This is further justified by the theoretical calculations of this study. Moreover, high temperature is essential for overcoming kinetic barriers. The detailed report of the theoretical investigation of the phase diagram of the  $C_xN_y$  compounds using evolutionary search (USPEX code<sup>21</sup>) is published in ref 22. In this paper, we present only the theoretical results which are relevant for the major topic of the paper (see Theoretical Methods in the Supporting Information). This work increases our understanding of the emerging field of high-pressure chemistry and opens a new route for the synthesis of superhard materials based on novel stoichiometries instead of the long-sought  $C_3N_4$ .

## RESULTS

We have performed LH experiments at various pressures using dedicated systems combined with Raman spectroscopy<sup>23</sup> and XRD.<sup>24</sup> Single-crystal graphite and high-pressure gas-loaded  $N_2$  (served also as a pressure medium) have been used as reagents (see Experimental Methods in the Supporting Information). From these runs (see Figure S1 and Table S1, for the full list of experimental runs), we observe that, for pressures below 45–50 GPa and above 70 GPa, diamond was the only product after quenching to room temperature. The maximum achieved temperatures were <3000 and 5000 K, respectively, as coupling of the laser radiation with the sample becomes progressively smaller once diamond forms, preempting the formation of C–N compounds. In contrast, laser heating between 50 and 70 GPa resulted in higher achievable temperatures (>7000 K) because of the runaway temperature increase due to formation of metallic carbon melt. These experiments must have produced metallic molten carbon as they reached temperatures well above the melting line of diamond at this pressure<sup>25</sup> (see Figure S1). No diamond formation has been observed in runs with successful C–N synthesis.

XRD patterns before LH at 55 and 65 GPa (Figure 2a) of two independent runs reveal two families of Bragg peaks: (i) high-pressure form of carbon (HP-C) and (ii)  $\epsilon$  or  $\zeta$  phases of molecular nitrogen.<sup>26,27</sup> In the case of experiments using an iridium ring, as a spacer to detach the carbon sample from the diamond anvil, additional diffraction peaks from iridium<sup>28</sup> have been observed; in contrast, no rhenium peaks (gasket material) have been observed with the recessed gasket configuration. Bragg peaks positions of HP-C before LH are in agreement with previous studies (Figure S2a, data of this study and ref 29). Moreover, the determined in this study EOS of  $N_2$  is in agreement with the previous studies (Figure S2b). The XRD pattern of quenched samples in the close vicinity of the laser-heated spot reveals the appearance of new intense Bragg peaks (Figure 2b), the decrease of the relative intensity of nitrogen related peaks and the disappearance of the broad intense HP carbon peaks. A slight ( $\approx$ 2–5 GPa) decrease of pressure was

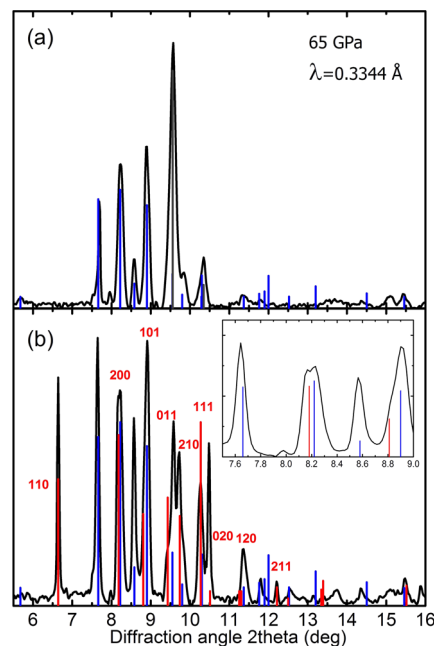


**Figure 2.** XRD patterns (a) before and (b) after LH at 65 GPa.  $\epsilon$ - $N_2$ , HP-C, and *Pnnm* CN peaks are marked with blue, gray, and red vertical lines, respectively. The  $2\theta$  position and the height of the vertical lines represent the expected (calculated) Bragg peaks positions and intensities, respectively. Calculations were performed, using the POWDERCELL program,<sup>30</sup> for the corresponding crystal structures according to the EOSs determined experimentally in this study and assuming continuous Debye rings of uniform intensity.

normally observed after LH. Remarkably, visual observation of the DAC indicates the presence of a transparent material exactly at the laser-heated spot (inset in Figure 3). Since no Bragg and Raman<sup>30</sup> peaks representative of diamond were observed, the observation of a transparent substance indicates the formation of a material other than diamond.

The Bragg peaks of the new phase can be well-indexed with an orthorhombic *Pnnm* (58) cell with  $Z = 4$  with  $a = 4.664 \text{ \AA}$ ,  $b = 3.664 \text{ \AA}$ , and  $c = 2.455 \text{ \AA}$  at 65 GPa (Figure 3). Moreover, we compared the experimental and the calculated patterns of the theoretically predicted phases with (a) 1:1 stoichiometry, including zincblende,<sup>14</sup> rocksalt,<sup>14</sup> body-centered tetragonal,<sup>14</sup>

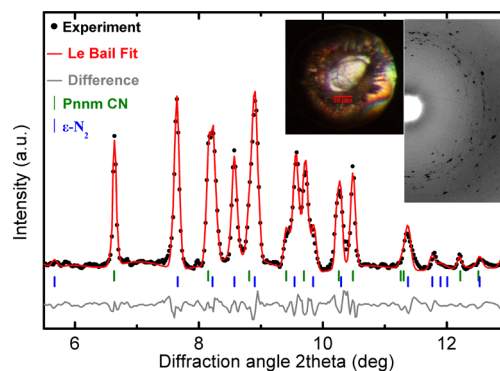


**Figure 3.** Le Bail refinement for CN at 65 GPa. *Pnnm* CN and  $\epsilon$ - $N_2$  peaks are marked with green and blue vertical lines, respectively. The X-ray wavelength is 0.3344 Å. The insets show (a) a microphotograph of the sample after heating in transmitted light, indicating the transparency of the synthesized phase, and (b) 2-D XRD image of the *Pnnm* CN and  $\epsilon$ - $N_2$  mixture.

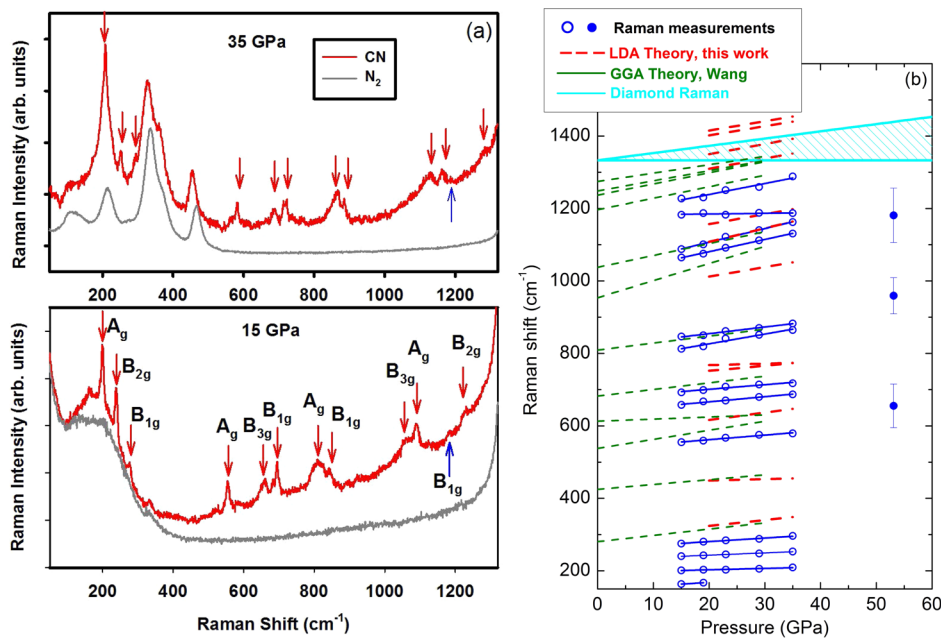


**Figure 4.** (a) Raman spectra at 15 and 35 GPa. Red curves correspond to CN and gray curves to molecular N<sub>2</sub>, measured in the same high-pressure cavity. The Raman peaks of *Pnnm* CN are marked by arrows: red arrows correspond to the peaks increasing (in frequency) with pressure and blue arrow pointing up to a weak peak decreasing with pressure. (b) Frequencies of Raman modes of *Pnnm* CN against pressure upon decompression. Experimental results with blue symbols and theoretically predicted with green (GGA<sup>18</sup>) and red (LDA this study) lines. The light blue area represents the frequency range dominated by Raman scattering of diamond. The error bars correspond to the bandwidth of broad Raman peaks, which were observed after the laser heating at 55 GPa.

cg-CN,<sup>17</sup> GaSe,<sup>15</sup> and  $\beta$ -InS<sup>15,18</sup> and (b) 3:4 stoichiometry, including  $\alpha$ -,  $\beta$ -, g-, cubic, and pseudocubic C<sub>3</sub>N<sub>4</sub>.<sup>1,2</sup> The almost perfect match, for all new peaks, can be observed in the case of the *Pnnm*  $\beta$ -InS-type structure (Figure 3 and Table S2), whereas there is no match with other predicted structures (see Figure S3). Representative Le Bail refinements of the experimentally observed diffraction patterns, after LH at the highest pressure for each run, based on the  $\beta$ -InS-type structure are shown in Figure 3 and Figure S4 for the separate synthesis at 65 (using a recessed gasket configuration) and 55 GPa, (using an iridium ring spacer), respectively. Preferred orientation effects and strongly anisotropic peak broadening effects (Figure 3, inset, and Figure S4b), which are usual in HP-HT synthesis, prevent us from a full structural refinement (Rietveld) of the positional parameters. According to the theoretical predictions, both carbon and nitrogen occupy 4g (*x,y,0*) Wyckoff positions with (0.355, 0.566, 0) and (0.816, 0.744, 0), respectively. Using these positional parameters we observe a fair agreement between calculated and observed intensities. To rule out the possible effect of different experimental configurations (Ir, Pt spacers, or recessed gasket) on the crystal structure and stoichiometry of the synthesized compound, we compared the XRD patterns of the independent synthesis at the same pressure (Figure S5). No difference, except of the relative intensity of Bragg peaks, has been observed, a result that indicates the absence of any influence of the experimental configurations on the synthesized compound. Moreover, XRD patterns collected at spacers positions and at the internal edge of the rhenium gasket hole revealed that no reaction between the spacers/gasket and nitrogen has occurred away from the laser-heated spot; i.e., only the Bragg peaks originating from hcp/fcc rhenium/iridium and N<sub>2</sub> were present.

Raman spectra (Figure 4a), of the new phase measured upon pressure release show a rich spectrum, characteristic of a low

symmetry cell. The lattice modes of N<sub>2</sub><sup>27</sup> can be readily separated as they are broader. The synthesized material remains stable on unloading, which was verified by XRD measurements; see below. Twelve Raman-active zone-center modes are predicted from group theory in the case of the *Pnnm* structure, with the symmetries: 4A<sub>g</sub> + 4B<sub>1g</sub> + 2B<sub>2g</sub> + 2B<sub>3g</sub>. Up to 13 narrow Raman bands have been observed in the quenched sample at low pressure, while 12 have been observed at pressures above 20 GPa and up to 35 GPa (Figure 4). A weak extra peak in the low-frequency spectral range, observed only below 20 GPa, cannot be explained at this point, but it can be an artifact (e.g., fluorescence) as the spectra are weak, position-dependent, and superimposed by a fluorescence. Above 35 GPa, the high-frequency CN modes interfere with the Raman signal of stressed diamond anvils; moreover, strong sample fluorescence did not allow obtaining high quality data at these conditions. The Raman bands observed at 15–35 GPa are grouped in three spectral regions in a remarkable qualitative agreement with the previously reported Raman spectra of InS (e.g., ref 31) as well as in a reasonably good match with the theoretically calculated Raman frequencies, given the fact that LDA usually overestimates the phonon frequencies (Figure 4). We tentatively assign the experimentally observed Raman modes following the results of the theoretical calculations (Figure S6). A plausible explanation of the moderate agreement between the calculated and observed Raman modes intensities is that the vibrational vectors are coupled (see Figure S6). Thus, the relative intensity of two or more modes of the same symmetry can vary depending on this coupling and may not be very well reproduced by theory. Moreover, the materials synthesized at extreme pressure–temperature conditions are highly textured (Figure 3, inset, and Figure S4b), which can distort the intensities.

The high-frequency modes of CN are expected to be below the C–C stretching region of diamond at a given pressure, since the C–C bond in *Pnnm* CN is slightly longer (1.57 Å) than that in diamond. All but one experimentally observed Raman modes show normal mode behavior with increasing pressure. A high-frequency weak C–C stretching mode, tentatively assigned to the  $B_{1g}$  mode (out-of-phase C–C stretching with simultaneous out-of-phase C–N bond stretching; see the Supporting Information, Figure S6), shows a redshift with increasing pressure. This can be understood as due to tilting of the C–C bond under pressure as discussed below. Overall, our Raman observations signify the presence of the C–N interatomic bonding and together with X-ray diffraction unequivocally identify the material as *Pnnm* CN. Comparison of the experimentally observed CN Raman modes with those reported in the case of PtN<sub>2</sub><sup>32</sup> and Re<sub>3</sub>N<sup>33</sup> (Figure S5b) further justifies the argument that no reaction products between the spacers/gasket and nitrogen are present in the area of the synthesized compound.

With decreasing pressure, the newly synthesized phase remains stable up to 12 GPa, as evidenced from XRD measurements and optical observations (Figure S7). Pressure dependence of the lattice parameters and volume per atom equation of state (EOS) of the *Pnnm* CN phase together with the theoretically predicted ones are shown in Figure 5. It is

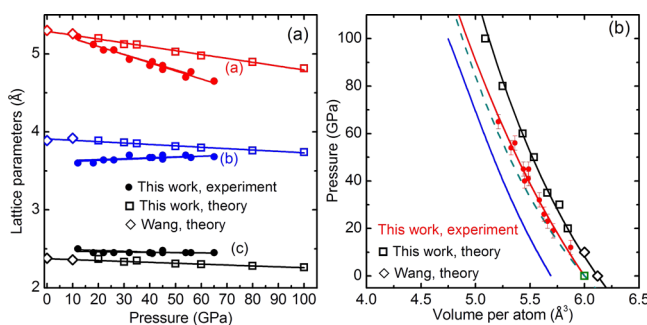


**Figure 5.** Pressure dependence of (a) lattice parameters and (b) volume per atom of *Pnnm* CN. Experimental data are shown with solid symbols and theoretical predictions with open ones. The solid curves in (b) are the third-order Birch EOS for diamond (blue) according to Zhu et al.,<sup>51</sup> the synthesized CN phase (red), and theoretical EOS predicted for *Pnnm* CN (black) according to this study and also Wang<sup>18</sup> and to Hart et al.<sup>15</sup> (green).

interesting to note a small negative compressibility along the *b* axis, which may be related to a similar observation in the  $\beta$ -InS compound under pressure.<sup>31</sup> This observation corroborates with the Raman mode softening (Figure 4), which is also similar to observations in ref 31. A plausible scenario of such anisotropic behavior is that the high compressibility of the *a* axis results in the tilting of the C–C dumbbells, with respect to the *a* axis (Figure 1d), so the C–C bond distance remains almost constant. Consequently, this results in an increase of the *b* axis. We have fitted the pressure–volume data by the third-order Birch equation of state<sup>34</sup> and determined the bulk modulus  $B_0$  and its first pressure derivative  $B'$ . The results of the fit are  $B_0 = 400$  (20) GPa,  $B' = 3.4$  (2), and  $V_0 = 6.04$  (3) Å<sup>3</sup>. The experimentally determined volume at ambient pressure is in a very good agreement with theoretically predicted ones (5.98 Å<sup>3</sup> by Hart et al.<sup>15</sup> and 6.12 Å<sup>3</sup> by Wang<sup>18</sup>). The synthesized material appears less compressible than predicted by Hart et al. (no  $B'$  value is given in this study, so a value of 4

is used for the EOS of Figure 5) but almost the same as predicted by Wang.<sup>18</sup> Therefore, the compressibility of the synthesized compound is comparable or even smaller than that of superhard *c*-BN.<sup>35</sup>

New Bragg peaks appear upon decompression below 12 GPa at 300 K in addition to the peaks from the *Pnnm* CN phase and the  $\delta$  phase of N<sub>2</sub> (Figure S8). These peaks cannot be attributed to the tetragonal *P4<sub>2</sub>/m* CN phase or the other previously proposed CN or C<sub>3</sub>N<sub>4</sub> phases. We have indexed these peaks with a monoclinic cell with a volume suggestive of a 4 formula unit cell in the case of 1:1 stoichiometry. Theoretical calculations revealed a monoclinic cell (SG *Pc* (7)  $Z = 4$ ), which has the same bonding configuration ( $sp^3$ -hybridized carbon; see Figure 1) as the previously proposed *Pnnm* and *P4<sub>2</sub>/m* phases, albeit with higher enthalpy. With further pressure release, both XRD Bragg and Raman peaks from the synthesized compound disappear below 6 GPa and the laser-heated spot becomes opaque. EDX spectroscopy of extracted samples reveals that a CN compound is preserved (Figure 6).

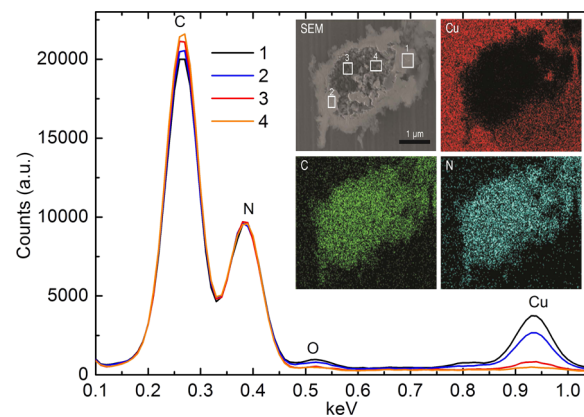


**Figure 6.** Representative EDX spectra, from different spots, of the CN compound at ambient conditions normalized to the N peak. The Cu and O peaks seen from spots close to the edge arise from the Cu foil used as a conducting substrate (see Experimental Methods). The inset shows an SEM/EDX micrograph and elemental maps of the surface of the recovered CN compound. Elemental analyses from the spots (not corrected for sample geometry) are summarized in Table 1.

We find that the composition of five recovered samples probed in different areas is consistent with the 1:1 stoichiometry. Variations in C/N (Table 1) are likely due to sample

**Table 1. Elemental Analyses from the Spots in Figure 6, Not Corrected for Sample Geometry<sup>a</sup>**

spectrum no.	C, at %	N, at %	C/N
1	54.57	45.43	1.20
2	55.02	44.98	1.22
3	55.43	44.57	1.24
4	55.67	44.33	1.26

<sup>a</sup>The overall uncertainty is <15%.

geometrical imperfections as well as to residual (unreacted) carbon in the X-ray extraction volume. It is plausible to assume that the unreacted carbon, away from the LH spot, was detected because of the EDX electrons diffusion (spreading of the electron beam) due to the low density of the extracted specimen (porous-like), the low-Z nature of the specimen, and the relatively low acceleration voltage used in this study.

Oxygen impurity may be due to organic contamination. A plausible scenario is that  $Pnnm$  CN becomes unstable below ca. 12 GPa with respect to decomposition to carbon and nitrogen, as predicted by the theoretical calculations of this study and also from previous theoretical studies.<sup>18,19</sup> However, instead of decomposing, because of kinetic barriers, it transforms to a metastable phase (monoclinic  $Pc$ ), while carbon remains in the  $sp^3$  bonding configuration. At lower pressures (<6 GPa), this metastable phase becomes dynamically unstable and eventually amorphizes,<sup>36,37</sup> keeping its (metastable) composition.

In order to examine the thermal effects on the stability of the CN  $Pnnm$ , we have performed Gibbs free energy calculations for various low relative enthalpy CN phases under variable temperature, in the 0–7000 K range, and pressure, in the 0–70 GPa range, conditions. As an example, we show in Figure S9a the results of our calculations at 55 GPa. The results of our calculations are summarized as follows: (a) The  $Pnnm$  is always the most stable phase from 0 K up to a critical temperature that ranges between  $\approx$ 1050 K at 0 GPa up to  $>$ 1700 K at 70 GPa. (b) Two alternative CN phases, namely,  $P4_2/m$  and  $Pbam$ , become more stable than the  $Pnnm$  phase above the critical temperature. These high-temperature phases are closely related to the  $Pnnm$  phase as they have the same bonding configuration ( $sp^3$ -hybridized carbon) and share common structural characteristics like the formation of 10- and 6-membered rings (see inset in Figure S9a). Although the possible formation of the HT phases is beyond the scope of this study, as the sample was rapidly quenched at RT and the melting line of the CN compounds is not known, it is plausible to assume that the high-temperature phases and the  $Pnnm$  phase are related through a temperature-induced phase transition. The comparison between the experimental pattern after LH at 65 GPa and the calculated pattern of the  $Pbam$  phase definitely rules out the possible formation of the, metastable at RT,  $Pbam$  phase (see Figure S9b).

## ■ DISCUSSION

Apart from the results of the XRD, Raman, and EDX measurements, the transparency of the material in the laser-heated spot, indicating a wide band gap material, are also in favor of synthesis of the  $\beta$ -InS-type CN phase. The electronic band structure of the various CN phases is determined by the carbon bonding configuration ( $sp^2$  or  $sp^3$ ).<sup>14</sup> Only crystal structures with  $sp^3$ -bonded carbon can be insulators,<sup>15</sup> whereas crystal structures with  $sp^2$ -bonded carbon (e.g., cg-CN) are expected to be metallic.<sup>17</sup> This is in a simple analogy with graphite and diamond. Thus, the transparency of the synthesized material can be used as an additional sample diagnostics. Indeed, our calculations,<sup>22</sup> as well as earlier theoretical predictions,<sup>18</sup> indicate that  $Pnnm$  CN has a wide band gap of 3.7 eV. Since single C–C bonds should only occur for  $sp^3$ -bonded carbon,<sup>14,15</sup> we conclude that the synthesized compound must have such bonds, which is an important ingredient for making this material superhard and additionally stabilizes the structure.

According to the theoretical results of this study (Figure 7a) and ref 22, above 14 GPa, CN compounds become thermodynamically stable with respect to decomposition into elemental carbon and nitrogen. Our experimental results indicate that higher pressure is needed for the successful formation of CN. This difference is not unusual (as in the case of graphite–diamond transformation), and moreover, at lower pressures, it may be difficult to achieve the necessary high

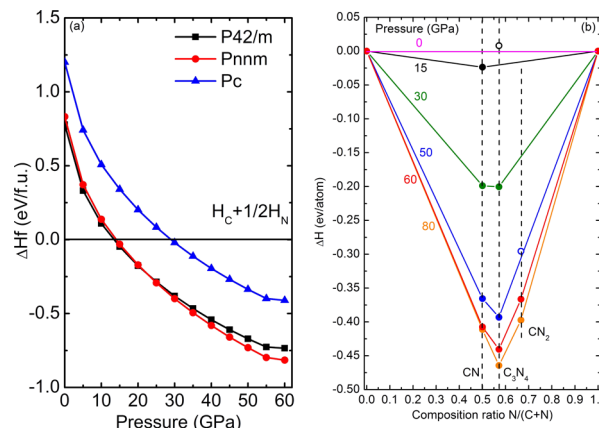


**Figure 7.** (a) Formation enthalpies per formula unit, determined by theoretical calculations of this study, relative to carbon and nitrogen as a function of pressure. Black, red, and blue curves correspond to the tetragonal  $P4_2/m$ , orthorhombic  $Pnnm$ , and monoclinic  $Pc$  CN phases, respectively. (b) Predicted convex hull diagrams of C–N system at selected pressures. Solid and open circles represent stable and metastable compounds, respectively.

temperatures for synthesis. Nevertheless, the convex hull diagram for the C–N system (Figure 7b) agrees with the experimental findings that the CN compound is stable (and  $C_3N_4$  is not) at pressures between the stability threshold (14 GPa) and the experimental synthesis pressure.

It is well-known that the correlation between bulk modulus, or even shear modulus ( $G$ ), which is considered more straightforward,<sup>38</sup> and material hardness ( $H$ ) is not direct and monotonic.<sup>39</sup> However, a high bulk modulus is usually, but not always, a strong indication of possible high hardness. During the past decade, substantial effort has been made<sup>39–41</sup> toward understanding the microscopic factors which determine hardness. The common consensus<sup>42</sup> is that high hardness depends on (a) shortness of bond length, (b) high number of bonds, (c) high number of valence electrons, and (d) high covalency of bonds. The CN  $Pnnm$  phase synthesized in this study satisfies all conditions and is superior in comparison to cubic BN due to lower ionicity.<sup>40,42</sup> Moreover, since metallic bonding always reduces hardness, due to the delocalized bonding,<sup>42</sup> the  $sp^3$  CN  $Pnnm$  phase (unlike metallic  $sp^2$ -bonded ones) we report in this study is the most promising one. Indeed, the theoretically calculated hardness, based on microscopic semiempirical models,<sup>39,41</sup> of  $\beta$ -InS-type CN determined as 59.6 GPa here, 62.3 GPa in ref 18, and 62.5 in ref 43 is comparable to that of superhard  $c$ -BN but less than that of diamond. Further studies are needed, such as of the stability of  $Pnnm$  CN at low temperatures and micro-hardness tests, which are precluded now because the synthesized material is not recoverable at ambient pressure–temperature conditions.

It is interesting to compare the results of our study with relevant “elemental” synthesis, using the same DAC-LH experimental configuration, of other compounds like the BN and  $B_2O_3$ . The main issue is whether, and to what extent, the mesoscopic state of the reactants has an influence on the stoichiometry of the obtained compounds<sup>44</sup> due to an increased ability of the liquid state to provide the constant supply of the element in the liquid state (lower melting temperature) within the laser-heated spot. In the case of the B–N system, the synthesis of  $h$ - and  $c$ -BN has been observed starting from elemental reagents at high pressure and temperature con-

ditions.<sup>45</sup> According to the known high-pressure melting lines of B<sup>46</sup> and N,<sup>47</sup> these conditions (e.g., 6.9 GPa, 1800 K) correspond to B and N in a solid and liquid state, respectively. However, only the known stoichiometric BN compound has been formed probably because a nitrogen-rich compound is not stable. In the case of the B–O system, the oxide with the maximum oxygen fraction has been synthesized,<sup>44</sup> i.e., B<sub>2</sub>O<sub>3</sub> instead of B<sub>6</sub>O (both being known stable compounds), at thermodynamic conditions corresponding to B and O in solid and liquid<sup>48</sup> states, respectively. This was attributed to the constant supply of oxygen within the laser-heated spot. From the previous discussion, it is plausible to conclude that the mesoscopic state of the reagents can influence the stoichiometry of the synthesized compound in the case that alternative stable stoichiometries (B–O system) exist; however, it cannot “induce” stoichiometries which are not stable (B–N system).

In the present study, we observe that a compound with lower N composition is formed, i.e., CN instead of C<sub>3</sub>N<sub>4</sub>. This result may have two origins: First, according to previous theoretical studies,<sup>14,15,17,18</sup> CN compounds with 1:1 stoichiometry are expected to be more stable than C<sub>3</sub>N<sub>4</sub>, mainly due to the increased N–N separation as such bonds are not energetically favorable.<sup>14</sup> Moreover, C<sub>3</sub>N<sub>4</sub> and sp<sup>3</sup> CN compounds, despite that C is in the sp<sup>3</sup> configuration in both of them, have a principal difference in bonding configuration: carbon atoms are connected with only nitrogens in the former one and with three nitrogens and one carbon in the latter one. The presence of strong C–C bonds is in favor to formation of thermodynamically stable material. This is further justified by the theoretical results of this study (Figure 7). The observation of a CN compound in a nitrogen-rich “environment” further justifies our experimental and theoretical findings that the 1:1 stoichiometry is more stable than the 3:4 one. Second, synthesis of the CN compound has been observed only at temperatures higher than the melting temperature of carbon at the corresponding pressure; that is, both reagents are in the liquid state. In this case, there is no difference in the mesoscopic state of the reagents and an almost unbiased synthesis takes place in a homogeneous nucleation reaction, as opposed to heterogeneous in the B–N and B–O systems, toward the most stable stoichiometry. At temperatures below the melting line of carbon, the existence of the extremely stable diamond phase imposes high kinetic barriers for the reaction and thus makes the melting of carbon a crucial precondition for the reaction between C and N.

Our combined experimental and theoretical study provides the first unambiguous evidence of a novel carbon nitride phase with a 1:1 stoichiometry where carbon atoms are in an sp<sup>3</sup> bonding configuration, forming a complete three-dimensional network. This *Pnnm* CN phase was synthesized at high pressure and high temperatures in the conditions where compounds with any (presumably the most stable) composition could be formed. Other previously predicted materials (e.g., C<sub>3</sub>N<sub>4</sub>) did not form, suggesting that they are metastable at these conditions. The CN *Pnnm* phase has all the necessary ingredients to be a prototype of a new family of superhard materials. This finding provides critical information for the search of new carbon nitride superhard materials with technological applications and also provides a crucial insight into the diverse chemical bonding of carbon under extreme conditions. Finally, it is noteworthy that our study underscores the importance of understanding the novel high-pressure chemistry laws. A number of previous investigations (e.g., ref

49) have concluded that 3D carbon nitrides are nonexistent material based on the fact that chemists never found a single hint of the existence of a covalent, single-bonded C–N network. In contrast, local C–N bonds are known to exist at ambient conditions, as in the case of monomeric heterocyclic compounds or in a 2D arrangement as in the case of g-C<sub>3</sub>N<sub>4</sub>. The results of this study reveal the formation of a network solid which has simultaneously C–C and C–N covalent bonds that indicate not only an unusual phase stoichiometry at high pressure and temperature conditions but also a completely new chemical behavior.

## ■ ASSOCIATED CONTENT

### S Supporting Information

The Supporting Information is available free of charge on the ACS Publications website at DOI: [10.1021/acs.chemmater.6b02593](https://doi.org/10.1021/acs.chemmater.6b02593).

Experimental methods, theoretical methods, and supporting figures and tables ([PDF](#))

## ■ AUTHOR INFORMATION

### Corresponding Authors

\*E-mail: [stavrou1@llnl.gov](mailto:stavrou1@llnl.gov) (E.S.).

\*E-mail: [agoncharov@carnegiescience.edu](mailto:agoncharov@carnegiescience.edu) (A.F.G.).

### Author Contributions

E.S., A.F.G., and A.R.O. designed the study; E.S., S.L., and A.F.G. performed the experiments and analyzed the experimental data; H.D. and A.R.O. performed the calculations; and Z.K. and V.B.P. performed experiments and contributed to the experimental methods.

### Notes

The authors declare no competing financial interest.

## ■ ACKNOWLEDGMENTS

E.S. thanks Karl Syassen for providing high quality natural graphite. S.L. thanks John Armstrong for technical assistance with SEM. This work was supported by the DARPA (grant No. W31P4Q1210008), the National Natural Science Foundation of China (Grant no. 21473211), and the Deep Carbon Observatory DCO. A.F.G. was partly supported by the Chinese Academy of Sciences visiting professorship for senior international scientists (Grant No. 2011T2J20) and Recruitment Program of Foreign Experts. S.L. was partly supported by the Ministry of Education and Science of Russian Federation (No. 14.B25.31.0032) and by state assignment project No. 0330-2014-0013. Part of this work was performed under the auspices of the U.S. Department of Energy by Lawrence Livermore National Security, LLC, under Contract DE-AC52-07NA27344. GSECARS is supported by the U.S. NSF (EAR-0622171, DMR-1231586) and DOE Geosciences (DE-FG02-94ER14466). Use of the APS was supported by the DOE-BES under Contract No. DE-AC02-06CH11357. The research leading to these results has received funding from the European Community's Seventh Framework Programme (FP7/2007-2013) under grant agreement no. 312284. Portions of this research were carried out at the light source PETRA III at DESY, a member of the Helmholtz Association (HGF).

## ■ REFERENCES

- (1) Liu, A.; Cohen, M. Prediction of New Low Compressibility Solids. *Science* **1989**, *245*, 841–842.

- (2) Teter, D.; Hemley, R. Low-Compressibility Carbon Nitrides. *Science* **1996**, *271*, 53–55.
- (3) Chen, Y.; Guo, L. P.; Wang, E. G. Experimental Evidence for Alpha- and Beta-phases of Pure Crystalline  $C_3N_4$  in Films Deposited on Nickel Substrates. *Philos. Mag. Lett.* **1997**, *75*, 155–162.
- (4) Niu, C.; Lu, Y. Z.; Lieber, C. M. Experimental Realization of the Covalent Solid Carbon Nitride. *Science* **1993**, *261*, 334–337.
- (5) Yu, K. M.; Cohen, M. L.; Haller, E. E.; Hansen, W. L.; Liu, A. Y.; Wu, I. C. Observation of Crystalline  $C_3N_4$ . *Phys. Rev. B: Condens. Matter Mater. Phys.* **1994**, *49*, 5034–5037.
- (6) Yin, L. W.; Li, M. S.; Liu, Y. X.; Sui, J. L.; Wang, J. M. Synthesis of Beta Carbon Nitride Nanosized Crystal through Mechanochemical Reaction. *J. Phys.: Condens. Matter* **2003**, *15*, 309.
- (7) Guo, Q.; Xie, Y.; Wang, X.; Lv, S.; Hou, T.; Liu, X. Characterization of Well-crystallized Graphitic Carbon Nitride Nanocrystallites via a Benzene-thermal Route at Low Temperatures. *Chem. Phys. Lett.* **2003**, *380*, 84–87.
- (8) Jürgens, B.; Irran, E.; Senker, J.; Kroll, P.; Muller, H.; Schnick, W. Melem (2,5,8-triamino-tri-s-triazine), an Important Intermediate During Condensation of Melamine Rings to Graphitic Carbon Nitride: Synthesis, Structure Determination by X-ray Powder Diffractometry, Solid-state NMR, and Theoretical Studies. *J. Am. Chem. Soc.* **2003**, *125*, 10288–10300.
- (9) Komatsu, T. Attempted Preparation of Diamond-like Carbon Nitride by Explosive Shock Compression of Poly(methineimine). *J. Mater. Chem.* **1998**, *8*, 2475–2479.
- (10) Liu, J.; Sekine, T.; Kobayashi, T. A New Carbon Nitride Synthesized by Shock Compression of Organic Precursors. *Solid State Commun.* **2006**, *137*, 21–25.
- (11) Zinin, P. V.; Ming, L. C.; Sharma, S. K.; Hong, S. M.; Xie, Y.; Irfune, T.; Shinmei, T. Synthesis of New Cubic  $C_3N_4$  and Diamond-like  $BC_3$  Phases Under High Pressure and High Temperature. *J. Phys.: Conf. Ser.* **2008**, *121*, 062002.
- (12) Kurakevych, O. O. Superhard Phases of Simple Substances and Binary Compounds of the B-C-N-O System: From Diamond to the Latest Results (a Review). *Journal of Superhard Materials* **2009**, *31*, 139–159.
- (13) Kojima, Y.; Ohfuchi, H. Structure and Stability of Carbon Nitride Under High Pressure and High Temperature up to 125 GPa and 3000 K. *Diamond Relat. Mater.* **2013**, *39*, 1–7.
- (14) Côté, M.; Cohen, M. L. Carbon Nitride Compounds with 1:1 Stoichiometry. *Phys. Rev. B: Condens. Matter Mater. Phys.* **1997**, *55*, S684.
- (15) Hart, J. N.; Claeysseens, F.; Allan, N. L.; May, P. W. Carbon Nitride: *ab initio* Investigation of Carbon-rich Phases. *Phys. Rev. B: Condens. Matter Mater. Phys.* **2009**, *80*, 174111.
- (16) Kim, E.; Chen, C. F.; Kohler, T.; Elstner, M.; Frauenheim, T. Tetragonal Crystalline Carbon Nitrides: Theoretical Predictions. *Phys. Rev. Lett.* **2001**, *86*, 652–655.
- (17) Wang, X.; Bao, K.; Tian, F.; Meng, X.; Chen, C.; Dong, B.; Li, D.; Liu, B.; Cui, T. Cubic Gauche-CN: A Superhard Metallic Compound Predicted via First-principles Calculations. *J. Chem. Phys.* **2010**, *133*, 044512.
- (18) Wang, X. Polymorphic Phases of  $sp^3$ -hybridized Superhard CN. *J. Chem. Phys.* **2012**, *137*, 184506.
- (19) Zhang, M.; Wei, Q.; Yan, H.; Zhao, Y.; Wang, H. A Novel Superhard Tetragonal Carbon Mononitride. *J. Phys. Chem. C* **2014**, *118*, 3202–3208.
- (20) Tomasino, D.; Chen, J.-Y.; Kim, M.; Yoo, C.-S. Pressure-induced Phase Transition and Polymerization of Tetracyanoethylene TCNE. *J. Chem. Phys.* **2013**, *138*, 094506.
- (21) Oganov, A. R.; Ma, Y.; Lyakhov, A. O.; Valle, M.; Gatti, C. Evolutionary Crystal Structure Prediction as a Method for the Discovery of Minerals and Materials. *Rev. Mineral. Geochem.* **2010**, *71*, 271–298.
- (22) Dong, H.; Oganov, A. R.; Zhu, Q.; Qian, G.-R. The Phase Diagram and Hardness of Carbon Nitrides. *Sci. Rep.* **2015**, *5*, 9870.
- (23) Goncharov, A. F.; Montoya, J. A.; Subramanian, N.; Struzhkin, V. V.; Kolesnikov, A.; Somayazulu, M.; Hemley, R. J. Laser Heating in Diamond Anvil Cells: Developments in Pulsed and Continuous Techniques. *J. Synchrotron Radiat.* **2009**, *16*, 769–772.
- (24) Prakapenka, V. B.; Kubo, A.; Kuznetsov, A.; Laskin, A.; Shkurikhin, O.; Dera, P.; Rivers, M. L.; Sutton, S. R. Advanced Flat Top Laser Heating System for High Pressure Research at GSECARS: Application to the Melting Behavior of Germanium. *High Pressure Res.* **2008**, *28*, 225–235.
- (25) Bundy, F. P.; Bassett, W. A.; Weathers, M. S.; Hemley, R. J.; Mao, H.-K.; Goncharov, A. F. The Pressure-temperature Phase And Transformation Diagram for Carbon; Updated Through 1994. *Carbon* **1996**, *34*, 141–153.
- (26) Olijnyk, H. High-pressure X-ray-diffraction Studies on Solid  $N_2$  up to 43.9 GPa. *J. Chem. Phys.* **1990**, *93*, 8968.
- (27) Gregoryanz, E.; Goncharov, A. F.; Sanloup, C.; Somayazulu, M.; Mao, H.-k.; Hemley, R. J. High P-T Transformations of Nitrogen to 170 GPa. *J. Chem. Phys.* **2007**, *126*, 184505.
- (28) Cerenius, Y.; Dubrovinsky, L. Compressibility Measurements on Iridium. *J. Alloys Compd.* **2000**, *306*, 26–29.
- (29) Wang, Y.; Panzik, J. E.; Kiefer, B.; Lee, K. K. M. Crystal Structure of Graphite under Room-temperature Compression and Decompression. *Sci. Rep.* **2012**, *2*, 520.
- (30) Hanfland, M.; Syassen, K.; Fahy, S.; Louie, S. G.; Cohen, M. L. Pressure Dependence of the First-order Raman Mode in Diamond. *Phys. Rev. B: Condens. Matter Mater. Phys.* **1985**, *31*, 6896–6899.
- (31) Schwarz, U.; Goncharov, A. F.; Syassen, K.; Gasanly, N. M. Structural Phase Transformation of InS at Higher Pressure. In *Joint XV AIRAPT and XXXIII EHPRG International Conference*, Warsaw, Poland, Sept 11–15, 1995.
- (32) Gregoryanz, E.; Sanloup, C.; Somayazulu, M.; Badro, J.; Fiquet, G.; Mao, H.-k.; Hemley, R. J. Synthesis and Characterization of a Binary Noble Metal Nitride. *Nat. Mater.* **2004**, *3*, 294–297.
- (33) Friedrich, A.; Winkler, B.; Refson, K.; Milman, V. Vibrational Properties of  $Re_3N$  from Experiment and Theory. *Phys. Rev. B: Condens. Matter Mater. Phys.* **2010**, *82*, 224106.
- (34) Birch, F. Finite Strain Isotherm and Velocities for Single-crystal and Polycrystalline NaCl at High-Pressures and 300k. *J. Geophys. Res.* **1978**, *83*, 1257–1268.
- (35) Goncharov, A. F.; Crowhurst, J. C.; Dewhurst, J. K.; Sharma, S.; Sanloup, C.; Gregoryanz, E.; Guignot, N.; Mezouar, M. Thermal Equation of State of Cubic Boron Nitride: Implications for a High-temperature Pressure Scale. *Phys. Rev. B: Condens. Matter Mater. Phys.* **2007**, *75*, 224114.
- (36) Deb, S. K.; Wilding, M.; Somayazulu, M.; McMillan, P. F. Pressure-induced Amorphization and an Amorphous-Amorphous Transition in Densified Porous Silicon. *Nature* **2001**, *414*, 528–530.
- (37) Ferlat, G.; Seitsonen, A. P.; Lazzeri, M.; Mauri, F. Hidden Polymorphs Drive vitrification in  $B_2O_3$ . *Nat. Mater.* **2012**, *11*, 925–929.
- (38) Brazhkin, V.; Dubrovinskaia, N.; Nicol, M.; Novikov, N.; Riedel, R.; Solozhenko, V.; Zhao, Y. From our Readers: What does 'Harder than Diamond' Mean? *Nat. Mater.* **2004**, *3*, 576–577.
- (39) Gao, F.; He, J.; Wu, E.; Liu, S.; Yu, D.; Li, D.; Zhang, S.; Tian, Y. Hardness of Covalent Crystals. *Phys. Rev. Lett.* **2003**, *91*, 015502.
- (40) Li, K.; Wang, X.; Zhang, F.; Xue, D. Electronegativity Identification of Novel Superhard Materials. *Phys. Rev. Lett.* **2008**, *100*, 235504.
- (41) Lyakhov, A. O.; Oganov, A. R. Evolutionary Search for Superhard Materials: Methodology and Applications to Forms of Carbon and  $TiO_2$ . *Phys. Rev. B: Condens. Matter Mater. Phys.* **2011**, *84*, 092103.
- (42) Oganov, A. R.; Lyakhov, A. O.; Zhu, Q. In *Comprehensive Hard Materials*; Sarin, V. K., Ed.; Elsevier: Oxford, 2014; Chapter 3.04, Theory of Superhard Materials, pp 59–79.
- (43) Tang, X.; Hao, J.; Li, Y. A First-principles Study of Orthorhombic CN as a Potential Superhard Material. *Phys. Chem. Chem. Phys.* **2015**, *17*, 27821–27825.
- (44) Nieto-Sanz, D.; Loubreyre, P.; Crichton, W.; Mezouar, M. X-ray Study of the Synthesis of Boron Oxides at High Pressure:phase

Diagram and Equation of State. *Phys. Rev. B: Condens. Matter Mater. Phys.* **2004**, *70*, 214108.

(45) Yoo, C. S.; Akella, J.; Cynn, H.; Nicol, M. Direct Elementary Reactions of Boron and Nitrogen at High Pressures and Temperatures. *Phys. Rev. B: Condens. Matter Mater. Phys.* **1997**, *56*, 140–146.

(46) Solozhenko, V. L.; Kurakevych, O. O. Equilibrium P-T Phase Diagram of Boron: Experimental Study and Thermodynamic Analysis. *Sci. Rep.* **2013**, *3*, 2351.

(47) Goncharov, A. F.; Crowhurst, J. C.; Struzhkin, V. V.; Hemley, R. J. Triple Point on the Melting Curve and Polymorphism of Nitrogen at High Pressure. *Phys. Rev. Lett.* **2008**, *101*, 095502.

(48) Weck, G.; Loubeyre, P.; Eggert, J. H.; Mezouar, M.; Hanfland, M. Melting Line and Fluid Structure Factor of Oxygen up to 24 GPa. *Phys. Rev. B: Condens. Matter Mater. Phys.* **2007**, *76*, 054121.

(49) Badzian, A.; Badzian, T.; Roy, R.; Drawl, W. Silicon Carbonitride, a New Hard Material and its Relation to the Confusion about Harder than Diamond  $C_3N_4$ . *Thin Solid Films* **1999**, *354*, 148–153.

(50) Kraus, W.; Nolze, G. POWDER CELL - a program for the representation and manipulation of crystal structures and calculation of the resulting X-ray powder patterns. *J. Appl. Crystallogr.* **1996**, *29*, 301–303.

(51) Zhu, Q.; Oganov, A. R.; Salvadó, M. A.; Pertíerra, P.; Lyakhov, A. O. Denser than Diamond: Ab Initio Search for Superdense Carbon Allotropes. *Phys. Rev. B: Condens. Matter Mater. Phys.* **2011**, *83*, 193410.